Are your MRI contrast agents cost-effective?
Learn more about generic Gadolinium-Based Contrast Agents.
FRESENIUS KABI
caring for life

AJNR

Quantitative Assessment of Variation in CT Parameters on Texture Features: Pilot Study Using a Nonanatomic Phantom

K. Buch, B. Li, M.M. Qureshi, H. Kuno, S.W. Anderson and O. Sakai

This information is current as of April 19, 2024.

AJNR Am J Neuroradiol 2017, 38 (5) 981-985
doi: https://doi.org/10.3174/ajnr.A5139
http://www.ajnr.org/content/38/5/981

Quantitative Assessment of Variation in CT Parameters on Texture Features: Pilot Study Using a Nonanatomic Phantom

K. Buch, B. Li, M.M. Qureshi, H. Kuno, S.W. Anderson, and O. Sakai

ABSTRACT

SUMMARY: Our aim was to evaluate changes in texture features based on variations in CT parameters on a phantom. Scans were performed with varying milliampere, kilovolt, section thickness, pitch, and acquisition mode. Forty-two texture features were extracted by using an in-house-developed Matlab program. Two-tailed *t* tests and false-detection analyses were performed with significant differences in texture features based on detector array configurations (*Q* values = 0.001–0.006), section thickness (*Q* values = 0.0002–0.001), and acquisition mode (*Q* values = 0.003–0.006). Variations in milliampere and kilovolt had no significant effect.

ABBREVIATIONS: GLCM = gray-level co-occurrence matrix; GLGM = gray-level gradient matrix; GLRL = gray-level run length; MDCT = multidetector row CT; RP = run percentage

Image texture describes a complex visual pattern within an image that consists of simpler subpatterns with characteristic features that may be evaluated through quantitative analysis known as a texture analysis.[1] Texture analysis is a set of quantitative, postprocessing, image-analysis algorithms that are being increasingly used within the field of radiology.[1-9] The texture analysis may be applied to any imaging technique including CT, MR imaging, and sonography, among others. The texture analysis is composed of a series of mathematic algorithms that extract texture descriptors from an image, thus allowing the mathematic detection of subtle changes in pixel intensity throughout an image.[1]

Within radiology, texture analysis has been used to detect subtle pathologic changes in an image that are not easily quantifiable by the human eye in a variety of areas of the body such as the liver, brain, and cartilage.[2-8] One of the most prevalent areas for use of texture analysis within radiology is for tumor evaluation and characterization.[8-18] Despite a growing number of publications on the use of texture analysis for tumor imaging, direct correlations between texture analysis features and histopathologic analysis are still being investigated.[18,19]

Recently, the upsurge in genomic discoveries and advanced imaging technologies on publicly available data bases, such as The Cancer Imaging Archive (http://www.cancerimagingarchive.net/) and The Cancer Genomic Atlas (https://cancergenome.nih.gov/), large, multi-institutional, quantitative genomic and imaging-based studies, are becoming areas of increased interest.[20,21] Particularly, within the field of tumor imaging, texture analysis is becoming increasingly used[8-18]; however, the lack of standardized scanning protocols poses a significant limitation to the use of texture analysis in these instances.

The purpose of this study was to evaluate how changes in CT parameters (milliampere, kilovolt[peak], section thickness, pitch, and acquisition mode) could affect variations in the texture analysis features irrespective of the internal architecture of the item being scanned.

MATERIALS AND METHODS

This study used a phantom for all image acquisitions, precluding the requirement for institutional review board approval.

Phantom Development

A nonanatomic phantom was constructed to investigate whether texture analysis features change with various CT parameters (milliampere, kilovolt[peak], section thickness, pitch, and acquisition mode). The phantom was constructed from a composition of cereal (Cheerios; General Mills, Minneapolis, Minnesota) and commercially available mayonnaise (Hellmann's; Unilever US, Englewood Cliffs, New Jersey). The content of the phantom was chosen on the basis of a regularly repeating geometric pattern composed of different internal densities, including air, fat, and grain (of

Received November 18, 2016; accepted after revision January 9, 2017.

From the Departments of Radiology (K.B., B.L., M.M.Q., H.K., S.W.A., O.S.), Radiation Oncology (M.M.Q., O.S.), and Otolaryngology–Head and Neck Surgery (O.S.), Boston Medical Center, Boston University School of Medicine, Boston, Massachusetts.

Please address correspondence to Osamu Sakai, MD, PhD, Department of Radiology, Boston Medical Center, Boston University School of Medicine, FGH Building, 3rd Floor, 820 Harrison Ave, Boston, MA 02118; e-mail: osamu.sakai@bmc.org

Indicates article with supplemental on-line appendix and tables.

http://dx.doi.org/10.3174/ajnr.A5139

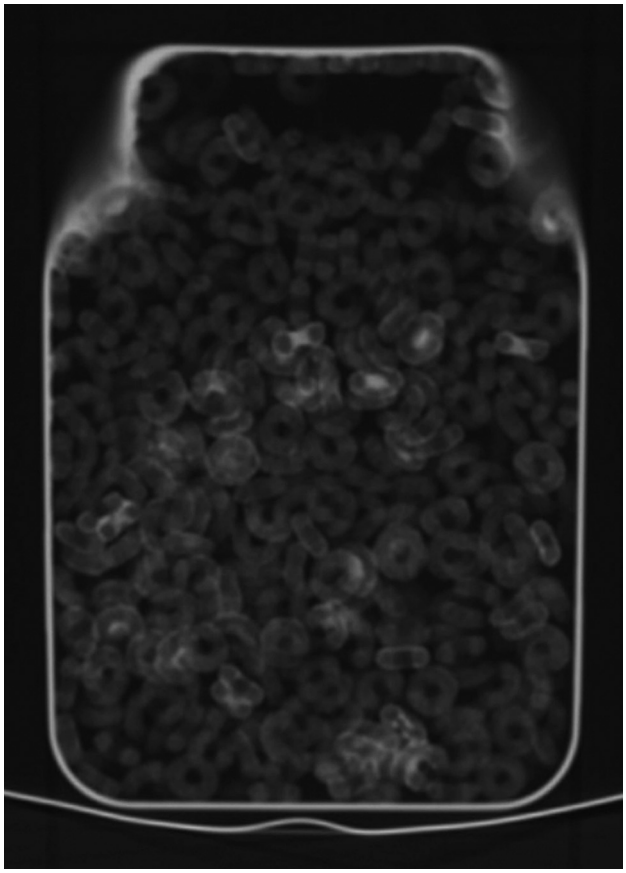

FIG 1. CT scan of the phantoms comprising Hellman's mayonnaise, Cheerios cereal, and air, housed in an acrylic container (15.88 × 23.50 × 31.75 cm).

slightly higher density). The phantom measured 15.88 × 23.50 × 31.75 cm (Fig 1).

CT Protocol

Noncontrast CT scans were obtained on the phantom on a 64–detector row CT scanner (Lightspeed VCT; GE Healthcare, Milwaukee, Wisconsin) and a 16–detector row CT scanner (LightSpeed, 16 section; GE Healthcare). In addition to scanning the phantom on different detector-row CT scanners, we also scanned the phantom with different CT parameters, including variations in the milliampere, kilovolt(peak), section thickness, and acquisition mode.

Each of the aforementioned CT scanning parameters was altered one at a time, while the remaining 5 texture features were held constant as shown in the Table.

The variations for the acquisition mode included an axial scan compared with a helical scan. Variations in milliampere ranged from 80 mA to 140 mA in increments of 20 mA. Similarly, variations in the kV ranged from 80 kV up to 140 kV in increments of 20 kV. Serial scans were obtained with variations in the thickness of the reconstructed axial datasets of 0.625, 1.25, 2.5, and 5 mm. Changes in helical pitch were also investigated by using pitches of 0.51, 0.98, 1.37, and 1.75.

Image Segmentation and Texture Analysis

The internal content of the phantom was manually contoured on an equal number of sections by a fourth-year diagnostic radiology resident on each CT scan. Segmentation was performed by using a dedicated workstation (Advantage Workstation; GE Healthcare) with a semiautomated graphical user interface.

Each contour was then imported into in-house-developed Matlab (MathWorks, Natick, Massachusetts) texture analysis software. The texture analysis software was developed by the coauthor (B.L.), and the use of this texture analysis program has been previously reported in the literature.[7,8] In total, 42 texture features, including 13 histogram features, 5 gray-level co-occurrence matrix (GLCM) features, 11 gray-level run-length (GLRL) features, 4 gray-level gradient matrix (GLGM) features, and 9 Law's features, were computed and averaged over the images per dataset.

The use of this in-house-developed Matlab program and the specific details of the texture analysis features calculated in this program have been previously published.[8] For additional details on the mathematic equations proposed by Haralick et al[1] and the GLRL matrix defined by Tang,[22] please refer to the On-line Appendix.

Outline of CT scanning protocol[a]

Varying Parameters	Scan No.	MDCT	Scan Type	Scan mA	Scan kV	Section Thickness	Pitch
MDCT	1	16	Axial	140	120	5	0.98
	2	64	Axial	140	120	5	0.98
	3	64	Axial	140	120	5	0.98
	4	64	Helical	140	120	5	0.98
Acquisition Mode	5	64	Helical	80	120	5	0.98
	6	64	Helical	100	120	5	0.98
Milliampere	7	64	Helical	120	120	5	0.98
	8	64	Helical	140	120	5	0.51
	9	64	Helical	140	80	5	0.98
	10	64	Helical	140	100	5	0.98
Kilovolt	11	64	Helical	140	120	5	0.98
	12	64	Helical	140	140	5	0.98
	13	64	Helical	140	120	5	0.51
	14	64	Helical	140	120	5	0.98
Pitch	15	64	Helical	140	120	5	1.37
	16	64	Helical	140	120	5	1.75
	17	64	Helical	140	120	0.625	0.98
	18	64	Helical	140	120	1.25	0.98
Section thickness	19	64	Helical	140	120	2.5	0.98
	20	64	Helical	140	120	5	0.98

[a] Eight CT scanning parameters were varied during serial CT acquisitions.

Statistical Analysis

The CT scanning parameters were incrementally changed, and the textures features were compared among the scans by using the Student *t* test for independent samples. To adjust for multiple comparisons, we performed a false discovery rate correction and calculated the false discovery rate–corrected *P* values (termed *Q* values) in addition to raw *P* values with the Benjamini-Hochberg method described in the literature.[23] Statistical computations were performed by using SAS 9.1.3 software (SAS Institute, Cary, North Carolina). The PROC MULTTEST function in SAS was used to calculate the *Q* values. A 2-tailed *P* value of $< .05$ was used to evaluate statistical significance.

RESULTS

The results of the texture analysis features with variations in CT parameters are shown in On-line Tables 1–8.

Multidetector Row CT Scanner

Significantly larger values were seen in the histogram features of second deviation ($P = .0042$, $Q = 0.018$) and range ($P = .0046$, $Q = 0.018$) as shown in On-line Table 1. There were no significant differences in the GLCM texture features with the exception of the texture feature correlation, which demonstrated lower values for the 64–multidetector row CT (MDCT) compared with 16–MDCT ($P = .012$, $Q = 0.039$). Overall, higher texture features were seen in all the Law's features for the 64–MDCT scanner compared with the 16–MDCT scanner (for all Law's features, $P < .0001$, $Q = 0.0005$). No statistically significant differences were seen in the GLRL or GLGM texture features.

Changes in Milliampere

All CT parameters except for milliampere were held constant on a 64–MDCT scanner. The milliampere varied from 80 to 140 mA in increments of 20 mA. For all included texture features, there were no statistically significant differences between the texture features based on the variations in the milliampere, as shown in On-line Table 1.

Changes in Kilovolt

All CT parameters except for kilovolt were held contrast for these serial scans of the phantom on the 64–MDCT scanner. Kilovolt varied from 80 to 140 kV in increments of 20 kV. For all included texture features, there were no statistically significant differences between the texture features based on the variations in kilovolt as shown in On-line Table 1.

Changes in Section Thickness

All CT parameters except for the section thickness were held constant for serial scans of the phantom on the 64–MDCT scanner. Serial helical acquisitions of the phantom were performed by using section thicknesses of 0.625, 1.25, 2.5, and 5 mm.

While there was no statistically significant difference in the histogram feature of mean ($P = .86$, $Q = 0.86$), statistically significant differences were seen in the other histogram features, including median ($P = .0004$, $Q = 0.0005$), SD ($P = .0006$, $Q = 0.0008$), second SD ($P < .0001$, $Q = 0.0002$), geometric mean ($P = .0013$, $Q = 0.0016$), and harmonic mean ($P < .0001$, $Q = 0.0002$), as shown in On-line Table 1. Additionally, all the GLCM texture features demonstrated statistically significant differences with variations in the section thicknesses.

Changes in Pitch

For variations in the pitch of helical scans, there were several significant differences in the Law's features of L5, L6, and L7 ($P = .021$, $P = .001$, $P = .0014$, respectively); however, after false discovery rate correction only the L6 feature remained statistically significant ($Q = 0.034$). No statistically significant differences were seen in the histogram, GLCM, GLRL, or GLGM texture features as shown in On-line Table 1.

Changes in Acquisition

Statistically significant differences were seen in the histogram features of second SD ($P = .0015$, $Q = 0.0045$) and range ($P = .0016$, $Q = 0.0045$), which exhibited lower values in an axial acquisition compared with a helical acquisition. No significant differences were seen in the GLCM features in an axial-versus-helical scan. Lower GLRL values were seen in the axial acquisition compared with the helical acquisition, with significant differences in the GLRL features of short-run emphasis ($P = .0024$, $Q = 0.63$), long-run emphasis ($P = .0006$, $Q = 0.0028$), gray-level nonuniformity ($P = .0011$, $Q = 0.0042$), and run-length nonuniformity ($P = .0007$, $Q = 0.0029$). No statistically significant differences were seen in the Law features or GLGM texture features shown in On-line Table 1.

DISCUSSION

The results of this study demonstrate statistically significant changes in the texture features based on the use of different CT parameters. CT texture features were not dependent on variations in milliampere and kilovolt. Variations in section thickness resulted in significant differences in the largest number of texture features, most of which were histogram texture features. To a lesser extent, the histogram features of second SD and range were both significantly affected by changes in the MDCT and an axial-versus-helical scan. Differences in CT texture features based on variations in scanning protocols have been suggested by the work of Fave et al[9]; however, to date, there remains no standardization for CT texture analysis or a comprehensive study investigating how CT parameters may influence the various texture parameters.

The use of texture analysis has been increasing in prevalence throughout the radiology literature, particularly as an adjunct aiding in diagnosis, lesion characterization, and even in the evaluation for treatment-related response.[10-14,19,24] Preliminary works investigating the use of a texture analysis to detect and characterize stages of hepatic fibrosis have been reported in the literature.[7,25,26] Similarly, texture analysis has also been used for examining potential differences in tissue architecture on CT in oropharyngeal squamous cell carcinomas and for help in evaluating changes in cartilage.[8,27] In these studies, a single CT protocol scanning algorithm has been used, limiting potential variations in the texture analysis feature related to scanning technique. This has future implications in multi-institutional research, such as for the imaging-based studies from The Cancer Imaging Archive, in which different scanning techniques could potentially reflect quantitative differences related to scanning techniques across different equipment manufacturers.

The GLCM texture features were most affected by changes in slice thickness. This dependency may be related to an increase in the likelihood of partial volume effect as the section thickness increases. Partial volume effect occurs when a structure partially intrudes the x-ray beam. With thicker sections, due to the volume-averaging effect, the contrast of the anatomy with its background decreases (ie, decreased GLCM contrast) and, visually, the image becomes more "homogeneous" (ie, increased GLCM homogeneity). Clinically, this is an important consideration because several GLCM features, particularly the GLCM texture feature of entropy, have been described as being important for tumor imaging.[15,16]

Multiple prior studies have highlighted the potential importance and ease of use of a quantitative texture analysis to evaluate

subtle changes in pixel intensity, which may not be evident to the human eye. The potential clinical applications of CT texture analysis include disease and lesion characterization, prognosis and treatment prediction, and treatment-response evaluation. However, a precise relationship between texture analysis features and a histopathologic understanding of correlative changes in tissue microstructure is less well-defined. Additionally, a prior study noted changes in texture features based on changes in CT parameters thought to reflect a degree of image heterogeneity.[17] In this study, we developed a physically heterogeneous phantom simulating varying densities to closely investigate how changes in CT scanning parameters influence texture analysis features. The impact of CT acquisition parameters on texture analysis features is an important consideration for the development and understanding of texture-based features when applied to CT images of clinical patients or research subjects. This is particularly important in cases in which texture analysis is used to evaluate treatment-related responses, longitudinal studies, and cross-institutional studies whereby the CT scanning parameters may vary, therefore further complicating the texture analysis results because measurements of image heterogeneity may be confused with biologic responses.

A previous study used a water phantom with no internal structural heterogeneity and concluded that the CT texture features were relatively insensitive to CT parameters such as tube voltage, tube current, and section thickness.[18] The results of this study also demonstrated that all examined texture analysis features were insensitive to tube voltage and tube current, but not scanning parameters or section thickness. The observed insensitivity of the texture features to changes in the tube voltage and current may reflect the phantom used in our study comprising similar material densities. Future investigation will be directed at using a more complex phantom with a greater variation in material densities. This study serves as an initial pilot investigation using a nonanatomic phantom looking into how differences in texture analysis features change with variations in CT parameters. The construction of additional phantoms with greater architectural complexity and composed of higher attenuation materials such as iodine, bone, and so forth is the next step in furthering our understanding of how material composition and CT techniques contribute to variations in texture analysis.

There are several limitations to this study. First, it used a nonanatomic phantom constructed of varying internal architecture of relatively low-density material. The texture results of this study would be most applicable to low-density soft-tissue and fat-attenuating structures. Higher attenuation material such as bone was not reflected in the design of this phantom. Future investigations will pursue an anatomic internal architecture, following this initial, pilot study. Second, a discrete range of varying milliampere, kilovolt, section thickness, and pitch was interrogated in this study; however, the ranges investigated may not be broad enough to cover a comprehensive range of all milliampere, kilovolt, section thickness, and pitch values used in radiology practices. Additionally, we chose to manually contour the internal content of our phantom for every study; that introduces a source of destandardization. Future work on this subject matter will entail an investigation into automated contouring to reduce any potential variation from manual contouring.

CONCLUSIONS

While texture analysis represents an increasingly popular, postprocessing, quantitative evaluation technique that can potentially be used as an adjunct in diagnostic imaging as a possible biomarker, standardization of CT parameters for the use of texture analysis is crucial to prevent features of intrinsic image heterogeneity from being confused with biologic features.

Disclosures: Hirofumi Kuno—*UNRELATED*: *Grants/Grants Pending*: Grant-in-Aid for Young Scientists (B) KAKEN (No. 26861033); *Payment for Lectures Including Service on Speakers Bureaus*: Toshiba Medical Systems. Osamu Sakai—*UNRELATED*: *Consultancy*: Guerbet, LLC, *Comments*: consulting fee; *Payment for Lectures Including Service on Speakers Bureaus*: Bracco Diagnostics.

REFERENCES

1. Haralick R, Shanmugam K, Dinstein I. **Textural features for image classification.** *IEEE Trans Syst Man Cybern A Syst Hum* 1973;SMC-3:610–21
2. de Carvalho Alegro M, Valotta Silva A, Yumi Bando S, et al. **Texture analysis of high-resolution MRI allows discrimination between febrile and afebrile initial precipitating injury in mesial temporal sclerosis.** *Magn Reson Med* 2012;68:1647–53 CrossRef Medline
3. Mayerhoefer ME, Stelzeneder D, Bachbauer W, et al. **Quantitative analysis of lumbar intervertebral disc abnormalities at 3.0 Tesla: value of T(2) texture features and geometric parameters.** *NMR Biomed* 2012;25:866–72 CrossRef Medline
4. Risse F, Pesic J, Young S, et al. **A texture analysis approach to quantify ventilation changes in hyperpolarised ^{3}He MRI of the rat lung in an asthma model.** *NMR Biomed* 2012;25:131–41 CrossRef Medline
5. Fujimoto K, Tonan T, Azuma S, et al. **Evaluation of the mean and entropy of apparent diffusion coefficient values in chronic hepatitis C: correlation with pathologic fibrosis stage and inflammatory activity grade.** *Radiology* 2011;258:739–48 CrossRef Medline
6. Jirák D, Dezortová M, Taimr P, et al. **Texture analysis of human liver.** *J Magn Reson Imaging* 2002;15:68–74 CrossRef Medline
7. Barry B, Buch K, Soto JA, et al. **Quantifying liver fibrosis through the application of texture analysis to diffusion weighted imaging.** *Magn Reson Imaging* 2014;32:84–90 CrossRef Medline
8. Buch K, Fujita A, Li B, et al. **Using texture analysis to determine human papillomavirus status of oropharyngeal squamous cell carcinomas on CT.** *AJNR Am J Neuroradiol* 2015;36:1343–48 CrossRef Medline
9. Fave X, Cook M, Frederick A, et al. **Preliminary investigation into sources of uncertainty in quantitative imaging features.** *Comput Med Imaging Graph* 2015;44:54–61 CrossRef Medline
10. Fried DV, Tucker SL, Zhou S, et al. **Prognostic value and reproducibility of pretreatment CT texture features in stage III non-small cell lung cancer.** *Int J Radiat Oncol Biol Phys* 2014;90:834–42 CrossRef Medline
11. Cunliffe AR, Armato SG 3rd, Straus C, et al. **Lung texture in serial thoracic CT scans: correlation with radiologist-defined severity of acute changes following radiation therapy.** *Phys Med Biol* 2014;59:5387–98 CrossRef Medline
12. Ba-Ssalamah A, Muin D, Schernthaner R, et al. **Texture-based classification of different gastric tumors at contrast-enhanced CT.** *Eur J Radiol* 2013;82:e537–43 CrossRef Medline
13. Ng F, Ganeshan B, Kozarski R, et al. **Assessment of primary colorectal cancer heterogeneity by using whole-tumor texture analysis: contrast-enhanced CT texture as a biomarker of 5-year survival.** *Radiology* 2013;266:177–84 CrossRef Medline
14. Schieda N, Thornhill RE, Al-Subhi M, et al. **Diagnosis of sarcomatoid renal cell carcinoma with CT: evaluation by qualitative imag-**

ing features and texture analysis. *AJR Am J Roentgenol* 2015;204:1013–23 CrossRef Medline
15. Lubner MG, Stabo N, Lubner SJ, et al. **CT textural analysis of hepatic metastatic colorectal cancer: pre-treatment tumor heterogeneity correlates with pathology and clinical outcomes.** *Abdom Imaging* 2015;40:2331–37 CrossRef Medline
16. Ahn SY, Park CM, Park SJ, et al. **Prognostic value of computed tomography texture features in non-small cell lung cancers treated with definitive concomitant chemoradiotherapy.** *Invest Radiol* 2015;50:719–25 CrossRef Medline
17. Ganeshan B, Miles KA. **Quantifying tumour heterogeneity with CT.** *Cancer Imaging* 2013;13:140–49 CrossRef Medline
18. Miles KA, Ganeshan B, Griffiths MR, et al. **Colorectal cancer: texture analysis of portal phase hepatic CT images as a potential marker of survival.** *Radiology* 2009;250:444–52 CrossRef Medline
19. Paniagua B, Ruellas AC, Benavides E, et al. **Validation of CBCT for the computation of textural biomarkers.** *Proc SPIE Int Soc Opt Eng* 2015;9417 CrossRef
20. Colen RR, Vangel M, Wang J, et al; TCGA Glioma Phenotype Research Group. **Imaging genomic mapping of an invasive MRI phenotype predicts patient outcome and metabolic dysfunction: a TCGA glioma phenotype research group project.** *BMC Med Genomics* 2014;7:30 CrossRef Medline
21. Kalpathy-Cramer J, Freymann JB, Kirby JS, et al. **Quantitative Imaging Network: data sharing and competitive algorithm validation leveraging The Cancer Imaging Archive.** *Transl Oncol* 2014;7:147–52 CrossRef Medline
22. Tang X. **Texture information in run-length matrices.** *IEEE Trans Image Process* 1998;7:1602–09 CrossRef Medline
23. Benjamini Y, Hochberg Y. **Controlling the false discovery rate: a practical and powerful approach to multiple testing.** *Journal of the Royal Statistical Society* 1995;57:289–300
24. Hodgdon T, McInnes MD, Schieda N, et al. **Can quantitative CT texture analysis be used to differentiate fat-poor renal angiomyolipoma from renal cell carcinoma on unenhanced CT images?** *Radiology* 2015;276:787–96 CrossRef Medline
25. Daginawala N, Li B, Buch K, et al. **Using texture analyses of contrast enhanced CT to assess hepatic fibrosis.** *Eur J Radiol* 2016;85:511–17 CrossRef Medline
26. Yu H, Buch K, Li B, et al. **Utility of texture analysis for quantifying hepatic fibrosis on proton density MRI.** *J Magn Reson Imaging* 2015;42:1259–65 CrossRef Medline
27. MacKay JW, Murray PJ, Kasmai B, et al. **MRI texture analysis of subchondral bone at the tibial plateau.** *Eur Radiol* 2016;26:3034–45 CrossRef Medline